Active Oceanic Spreading in the Northern North Fiji Basin: Results of the NOFI Cruise of R/V *L'Atalante* (Newstarmer Project)

YVES LAGABRIELLE[1], ETIENNE RUELLAN[2], MANABU TANAHASHI[3], JACQUES BOURGOIS[4], GEORGES BUFFET[2], GIOVANNI de ALTERIIS[1], JÉRÔME DYMENT[1], JEAN GOSLIN[1], EULÀLIA GRÀCIA-MONT[1], YO IWABUSHI[5], PHILIP JARVIS[6], MASATO JOSHIMA[3], ANNE-MARIE KARPOFF[7], TAKESHI MATSUMOTO[8], HÉLÈNE ONDRÉAS[9], BERNARD PELLETIER[10], and OLIVIER SARDOU[2]

[1] *CNRS/Université de Bretagne Occidentale, URA 1278 "Domaines Océaniques" and GDR 910, 6 av. Le Gorgeu, BP 809, F-29285 Brest Cedex, France*
[2] *Institut de Gèodynamique, URA 1279 CNRS-UNSA, 250 rue Albert Einstein, Sophia Antipolis, F-06560 Valbonne, France*
[3] *Geological Survey of Japan, Marine Geology Department, 1-1-3 Higashi, Yatabe, Tsukuba, Ibaraki 305, Japan*
[4] *CNRS / Université P. & M. Curie, Paris 6, URA 1315, Bte 119, 4 place Jussieu, 75252 Paris Cédex 05, France*
[5] *Japan Hydrographic Department, Maritime Safety Agency, 5-3-1, Tsukiji Chuo, Tokyo 104, Japan*
[6] *University of Tokyo, Ocean Research Institute (ORI), 1-15-1, Minamidai, Nakano-Ku, Tokyo 164, Japan*
[7] *CNRS – UPR 6251, Centre de Géochimie de la Surface, 1 rue Blessig, F-67084 Strasbourg Cedex, France*
[8] *JAMSTEC, 2-15, Natsushima-Cho, Yokosuka 237, Japan*
[9] *IFREMER – Centre de Brest, DRO-GM, BP 70, F-29280 Plouzane Cedex, France*
[10] *ORSTOM – UR 14 Géologie-Géophysique, BP A5, Noumea Cedex, Nouvelle Caledonie*

(Received 10 April 1995; accepted 9 August 1995)

Key words: North Fiji basin, back-arc basins, spreading centers, segmentation, axial grabens, axial volcanic highs

Abstract. The South Pandora and the Tripartite Ridges are active spreading centers located in the northern part of the North Fiji Basin. These spreading centers were surveyed over a distance of 750 km during the NOFI cruise of R/V *L'Atalante* (August-September 1994) which was conducted in the frame of the french-japanese Newstarmer cooperation project. *SIMRAD EM12-dual* full coverage swath bathymetric and imagery data as well as airgun 6-channel seismic, magnetics and gravity profiles were recorded along and off-axis from 170°40′ E to 178° E. Dredging and piston coring were also performed along and off-axis. The axial domain of the South Pandora Ridge is divided into 5 first-order segments characterized by contrasted morphologies. The average width of the active domain is 20 km and corresponds either to bathymetric highs or to deep elongated grabens. The bathymetric highs are volcanic constructions, locally faulted and rifted, which can obstruct totally the axial valley. The grabens show the typical morphology of slow spreading axes, with two steep walls flanking a deep axial valley. Elongated lateral ridges may be present on both sides of the grabens. Numerous volcanoes, up to several kilometers in diameter, occur on both flanks of the South Pandora Ridge. The Tripartite Ridge consists of three main segments showing a sigmoid shape. Major changes in the direction of the active zones are observed at the segment discontinuities. These discontinuities show various geometrical patterns which suggest complex transform relay zones. Preliminary analysis of seismic reflection profiles suggest that the Tripartite Ridge is a very young feature which propagates into an older oceanic domain characterized by a significant sedimentary cover. By contrast, a very thin to absent sedimentary cover is observed about 100 km on both flanks of the South Pandora Ridge active axis. The magnetic anomaly profiles give evidence of long and continuous lineations, parallel to the South Pandora Ridge spreading axis. According to our preliminary interpretation, the spreading rate would have been very low (8 km/m.y. half rate) during the last 7 Ma. The South Pandora and Tripartite Ridges exhibit characteristics typical of active oceanic ridges: (1) a segmented pattern, with segments ranging from 80 to 100 km in length; (2) an axial tectonic and volcanic zone, 10 to 20 km wide; (3) well-organized magnetic lineations, parallel to the active axis; (4) clear signature on the free-air gravity anomaly map. However, no typical transform fault is observed; instead, complex relay zones are separating first-order segments.

Marine Geophysical Researches **18:** 225–247, 1996.

1. Introduction: Objectives of the NOFI Cruise

Recent detailed surveys of mid-oceanic ridges with various spreading rates in wide oceans as well as in back-arc basins have shown that the geometry and the axial morphology of the active axis may be unstable with a periodicity of the order of 1 My (Macdonald, 1986; Gente, 1987; Semperé *et al.*, 1990; Fox *et al.*, 1991; Macdonald *et al.*, 1992; Palmer *et al.*, 1993). This instability is revealed by non-linear active axes made of short segments with poorly organized relay zones, frequent discontinuities and changes of trend. Segments with axial depressions pass abruptly to segments showing flat or dome-like sections lacking sommital graben.

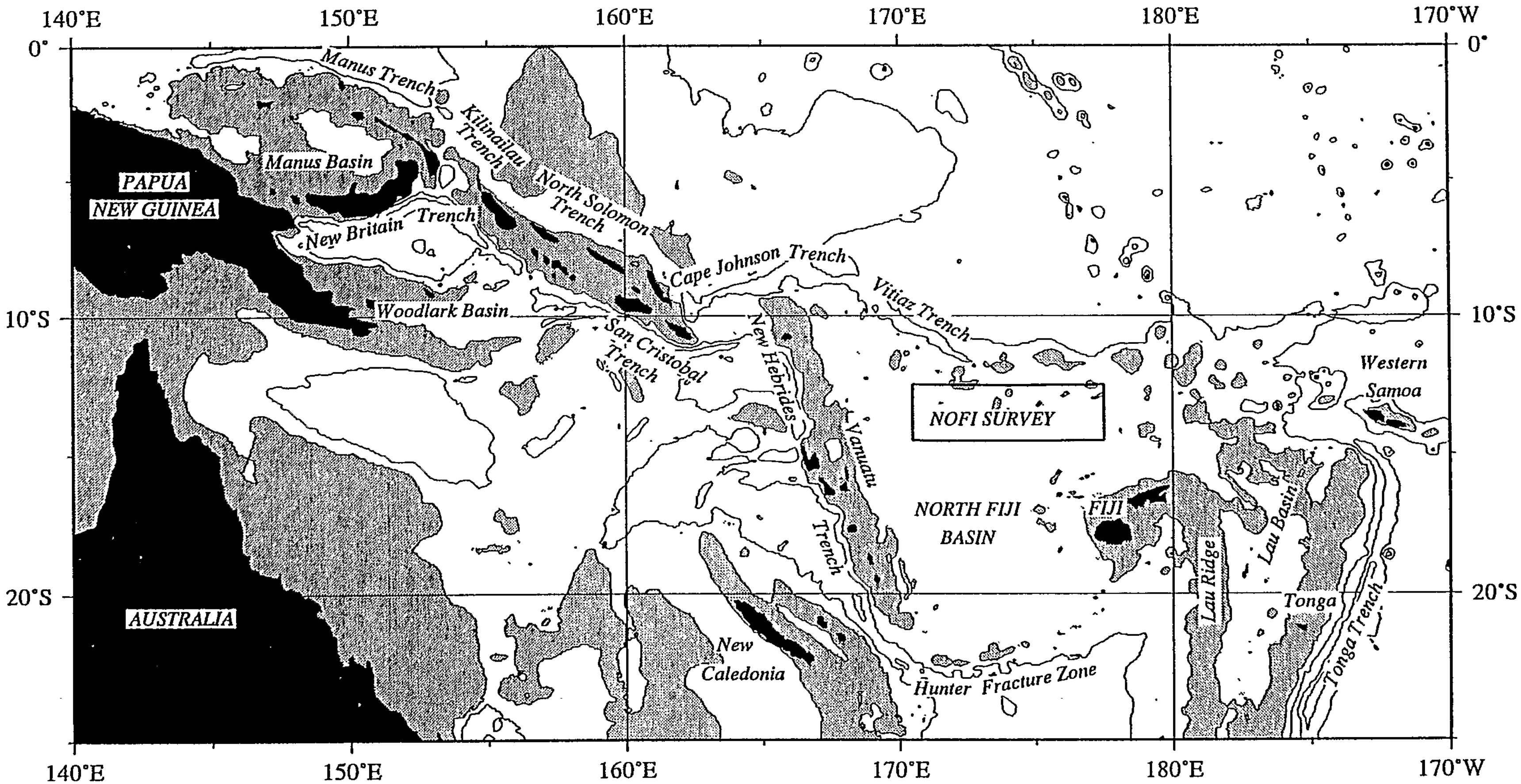

Figure 1. General map of the Southwest Pacific and location of the NOFI survey in the North Fiji Basin.

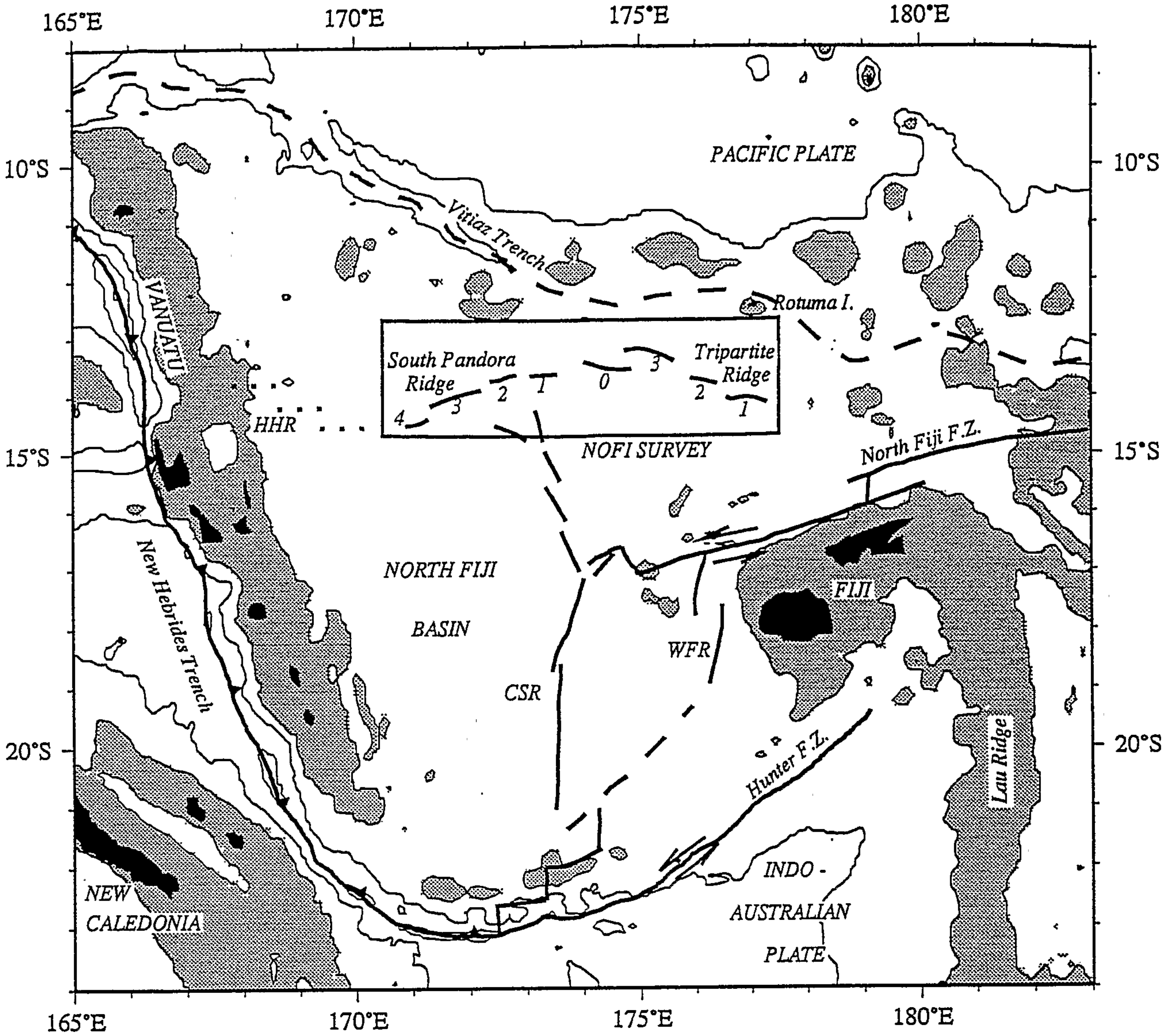

Figure 2. Structural sketch showing the main active features of the North Fiji Basin. Solid lines indicate well-defined active plate boundaries, dashed lines inactive or uncertain boundaries. CSR: Central Spreading Ridge, WFR: West Fiji Ridge, HHR: Hazel Holmes Ridge. Numbers refer to the successive segments of the South Pandora and Tripartite Ridges (see text).

Such variability in the geometry of active spreading systems has been well documented in the North Fiji Basin (NFB hereafter), one of the more evolved back-arc basins in the world (Figure 1; Auzende *et al.*, 1988a; Auzende *et al.*, 1988b; Louat and Pelletier, 1989; de Alteriis *et al.*, 1993; Gracia *et al.*, 1994; Ruellan *et al.*, 1994; Tanahashi *et al.*, 1994; Gracia *et al.*, this issue). Surveys conducted during the last 12 years have revealed a complex geometry of the NFB spreading centers (Figure 2). The active system is composed of a main central ridge, the Central Spreading Ridge consisting itself of successive segments with various orientations, showing opposite dome-shaped and graben-shaped morphologies. The Central Spreading Ridge is connected through the North Fiji Fracture Zone to a subordinate, east–west spreading system (the West Fiji Ridge or Wiva Rift, Figure 2) consisting of a twin, arcuate axis (Huchon *et al.*, 1994; Auzende *et al.*, 1994).

The northern region of the NFB was poorly known before the NOFI cruise. Active spreading centers with a broad E–W orientation were supposed to exist along the South Pandora Ridge (SPR hereafter) and the Tripartite Ridge (TR hereafter), but little was known about their detailed geometry, morphotectonic pattern, geophysical characteristics and petrological evolution. New data from this region were needed in order to better understand the geometry and recent evolution of the spreading systems, their connection with the Central Spreading Ridge, and finally the kinematics of the entire NFB.

The operations conducted during the NOFI cruise included *SIMRAD EM12-dual* swath bathymetric and acoustic imagery mapping (Plates A and B) and underway geophysics (airgun 6-channel seismics, magnetics and gravity profiling) in the northern part of the NFB between 171° E–178° E and 13° S–15° S (Figure 3). The profiles were navigated to complete a 100% coverage map located between 170°45′ E–175°30′ E and 13° S–15° S, over an area of extension 600 km along-axis and 120 to 200 km across-axis (Figure 4). Widely spaced 'zig-zag' profiles were navigated across the TR and the Rotuma Ridge, a volcanic ridge trending N 80°, in the east of the survey area, resulting in a 20/25%-coverage map of a 240 × 230 km area between 174°–177°45′ E and 12°30′–14°40′ S.

One piston core was taken in an off-axis basin (NF-C1), three dredges were obtained within the active axis of the South Pandora Ridge (NF-DR1, NF-DR2, NF-DR7), one dredge was taken between the ridge axis and Horizon Bank (NF-DR6), and another one off-axis, on the flank of a large volcano (NF-DR3) (Figure 5). Finally, two dredges and one piston-core were taken near the junction between the TR and the SPR (NF-DR4, NF-DR5 and NF-C2) (Figure 6).

2. Geological Framework and Previous Work in the South Pandora-Tripartite Ridges Region

The SPR was considered part of the so-called "Hazel Holme Fracture Zone" (Chase, 1971) (Figure 2). It consists of a broad, complex arch, trending globally east–west showing a strong linear fabric. The existence of an active spreading center in the Northern North Fiji basin was first proposed from the analysis of magnetic anomalies (Lapouille, 1986). On the bathymetric map published by Kroenke *et al.* (1994), the SPR appears as a pair of ridges flanking an axial trough, all of which clearly undergo several offsets. The strong east–west linear fabric of the SPR has been observed over limited detailed SeaMARC and GLORIA surveys (Price and Kroenke, 1991; Tiffin *et al.*, 1991; Jarvis *et al.*, 1993; 1994). Extremely young glassy lavas, described as alkali-enriched tholeiites or "transitional" basalts (Seward, 1994), have been recovered at different locations in the northern NFB, more particularly along the axes of the SPR and TR (Kroenke *et al.*, 1987; Price *et al.*, 1990; Price and Kroenke, 1991; Von Stackelberg and Von Rad, 1990; Kroenke *et al.*, 1994).

Finally, the SPR has been interpreted as an active spreading center, on the ground that (a) it is seismically active; (b) bathymetry and gravity profiles are similar to those obtained across other well-surveyed spreading centers, more particularly across slow-spreading ones (Kellog and Kansakar, 1994); (c) fresh to very fresh pillow basalts have been dredged along the ridge at several locations (Kroenke *et al.*, 1994).

The TR is an elongated feature, trending N110° E and has also been interpreted by Kroenke *et al.* (1994) as a very young spreading axis. It was explored in detail very locally in the region of Cakabau Seamount during a SeaMARC II survey in 1987 (Price *et al.*, 1990; Price and Kroenke, 1991).

The Rotuma Ridge is a line of volcanic seamounts trending N 80° E, along which depths as shallow as 1000 m are observed, bounded by two 3000-m-deep parallel troughs. The Rotuma Ridge and the TR connect to the eastern end of the SPR at 175° 30′ E. The Island of Rotuma, located at the eastern tip of the Rotuma Ridge, exposes very fresh alkaki-olivine basalts and hawaiite of Late Pleistocene and Recent age (Woodhall, 1987).

Relatively few dense geophysical surveys were conducted over the northern NFB prior to the NOFI cruise. Kellog and Kansakar (1994) produced a free-air anomaly map in the Northern Fiji Basin, in an area located between 12° S–17° S and 171° E–176° E and contoured the Bouguer anomaly computed along ship tracks. Minima over several segments of the SPR were interpreted as indicative of slow spreading along this axis. Moreover, they interpreted the isostatic compensation of near-ridge volcanoes as favouring their emplacement on a weak and therefore young plate, another argument in favour of the occurrence of active spreading along the SPR. Finally, the regional trend of the free-air anomaly, decreasing eastward away from the New Hebrides Trench has been interpreted as reflecting the influence of deeply subducted lithospheric fragments.

An aeromagnetic survey was flown radially from Viti Levu and interpretated in several papers (Malahoff *et al.*, 1979; Cherkis, 1980; Larue *et al.*, 1982; Auzende *et al.*, 1988b). These data show the existence of seafloor spreading anomalies in the northern part of the basin (Malahoff *et al.*, 1994; Pelletier *et al.*, 1993b). However, the identification of these anomalies, also evidenced on a map based on shipboard measurements (Pelletier *et al.*, 1993b; Malahoff *et al.*, 1994) remains somewhat unreliable. The magnetic anomaly pattern nevertheless indicated an en echelon structure for the

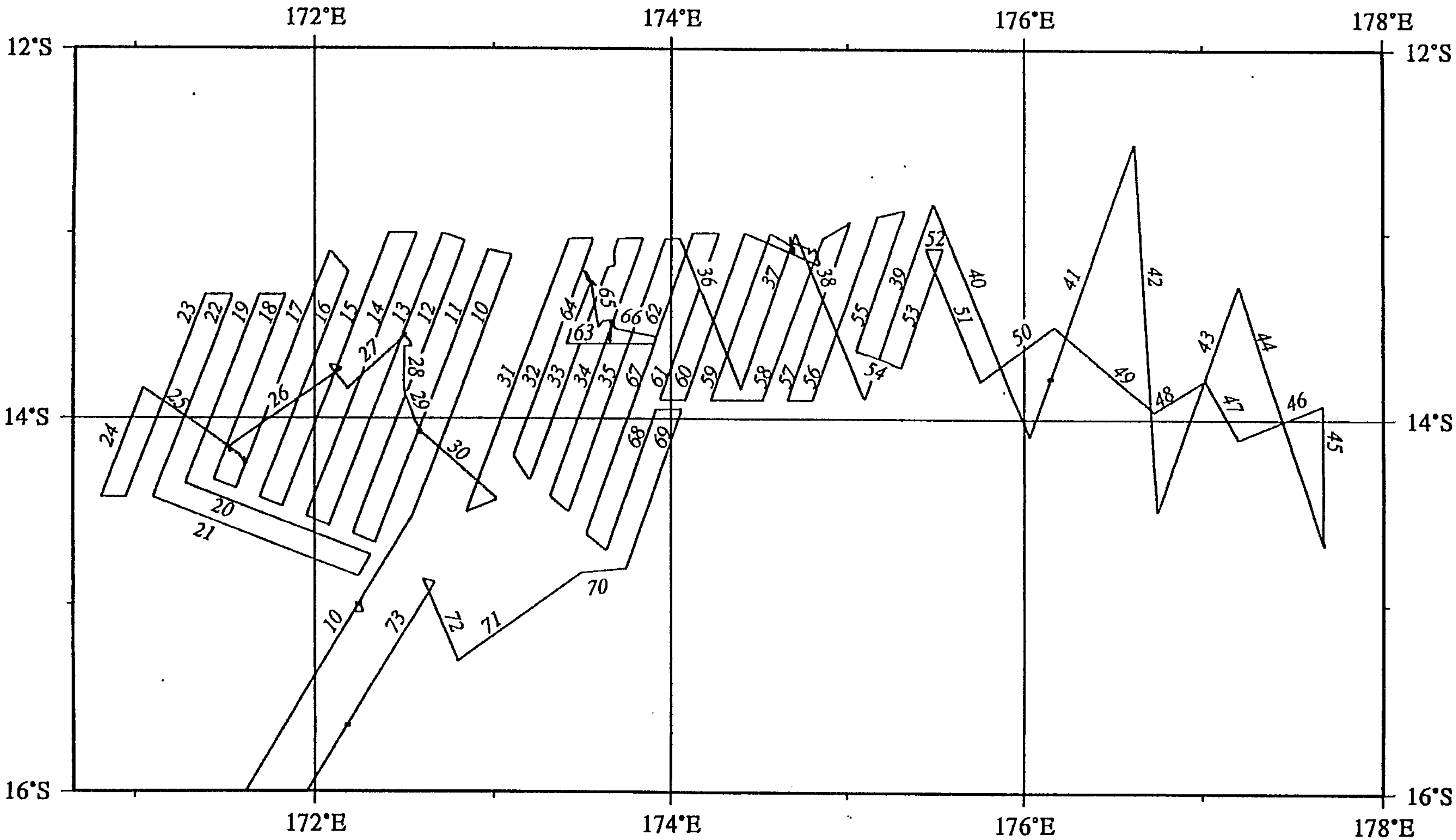

Figure 3. Location of ship's tracks sailed during the NOFI cruise.

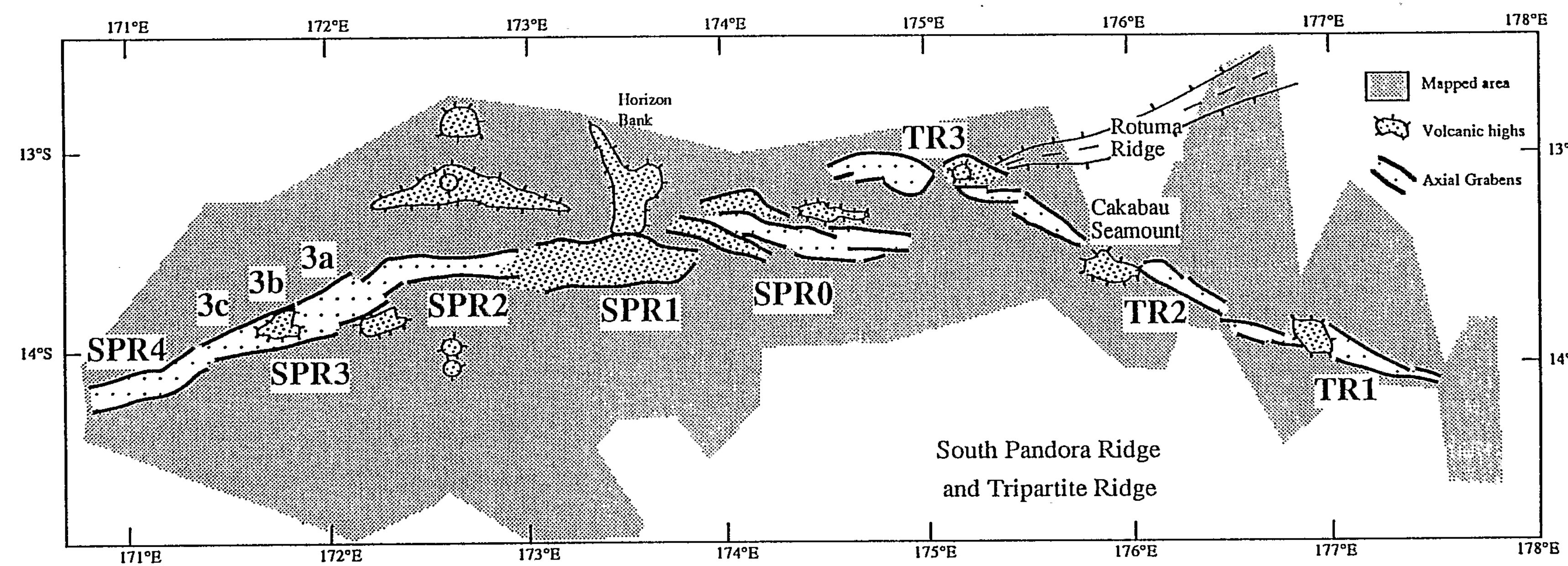

Figure 4. Simplified sketch of the South Pandora and Tripartite Ridges active spreading system. SPR0-4 and TR1-3 refer to ridge segments discussed in the text. The shaded area represents the bathymetry and imagery coverage of the NOFI cruise.

western portion of the SPR, while the relations between this ridge and the Hazel Holmes Extension Zone remained not clearly understood.

The analysis of shallow focal mechanisms (Eguchi, 1984; Louat and Pelletier, 1989; Hamburger and Isacks, 1988; 1994) indicates that strike slip mechanisms are dominant over the northern NFB. Hamburger and Isacks (1988) proposed a model of "diffuse extension" to account for the paucity of normal faulting mechanisms and for the dispersion of epicenters throughout the area, in some contradiction with the presence of an active spreading center.

3. First Results of the NOFI Cruise

3.1. Bathymetry-Imagery Data

3.1.1. Geometry and structure of the SPR active axial domain

The SPR and TR axial domains are characterized by high-reflectivity terranes forming an E–W oriented broad arch observed continuously along the mapped area (Plate B). From 170°40′ to 172°20′ E, the global trend of the axial zone is N 70° E (with a change in direction at 171°20′ E), and becomes N 90° E east of 172° 20′ E .

The average width of the active domain is 20 km and corresponds either to bathymetric highs or to deep elongated grabens located on top of the regional dome forming the SPR. The bathymetric highs are locally faulted and rifted volcanic constructions, which can obstruct totally the axial valley. The grabens show the typical morphology of slow-spreading rifted axes, with two steep walls flanking a 10 to 20-km wide and more than 1000-m deep axial valley. Lateral volcanic ridges are present on both sides of the graben. Elongated ridges, interpreted as neovolcanic ridges, are locally observed within the axial valley itself.

According to bathymetry and imagery analysis, the axial domain can be divided into five first-order segments, named SPR0 to SPR4 from east to west (Figure 4).

Axial segmentation (Figure 5). The E–W trending segment SPR0 is a 100 km-long and 4100 m-deep graben. At its western tip the graben is bounded by two symmetrical elongated highs between which a neovolcanic ridge can be observed.

Segment SPR1 is characterized by the presence of a very large axial volcanic high (Figure 7, line NF-10) shallowing to 1200 m depth. This high is rifted by two sets of faults trending N 90° E and N 100° E–110° E which define a rhomboidal fabric. A median valley trending N 100° E separates the segment into two main parts. In the western part, the axial high is bounded by two E–W elongated valleys. In its eastern part, the volcanic high connects northward to the 'Horizon Bank' through a north–south trending ridge.

Segment SPR2 shows a bathymetric transverse section similar to those of slow-spreading ridges (Figure 7, lines NF-11 and NF-12). It consists of an E–W trending graben flanked by two sharp lateral-ridges. The average depth of the axial valley floor varies from 2400 m to 4200 m. E–W trending neovolcanic ridges, 200 to 300 m high and 20 to 35 km long are observed at the foot of the valley walls. These internal ridges show lateral offsets of ten kilometres. Two of them are located close to the southern wall, the median one, which is also the longest, is located at the base of the northern wall. A second-order segmentation can be defined by the position of these internal ridges, which coincides with offsets of the graben walls.

Segment SPR3 is oriented N 75° E, thus marking a clear change in the trend of the SPR. It is composed of a deep graben passing laterally into a median volcanic high. Its total length is 120 km and it is bounded by two sharp ridges which can be interpreted as narrow horsts limited by vertical faults (Figure 8, lines NF-15 to NF-19).

Three second-order segments, oriented N 90° E, can be defined within segment SPR3 (segments SPR3a, SPR3b and SPR3c) (Figures 4 and 5), making up an 'en echelon' pattern:

1. Segment SPR3a consists of a N 75° E trending graben, which includes a secondary deep axial graben, trending N 90° E. At the eastern tip of the secondary graben was recorded the deepest sounding of the NOFI cruise, at the location of dredge NF-DR1 ("Nofi Deep" : 4787 m).
2. Segment SPR3b is characterized by a volcanic massif protruding within the axial domain and passing abruptly along axis into two grabens which end the segment to the East and West. The central volcanic high is rifted by faults trending N 90° E and N 75° E. A tectonic valley oriented N 90° E cuts through the middle of the eastern flank of the central massif.
3. Segment SPR3c consists of a main graben, characterized by the occurrence of an arcuate, secondary graben with a maximum depth of 4000 m, located in the axial part of the segment. This arcuate shape results of the interaction of tectonic directions N 90° E and N 75° E.

Segment SPR4 is located at the western edge of the survey area and has not been mapped completely, as

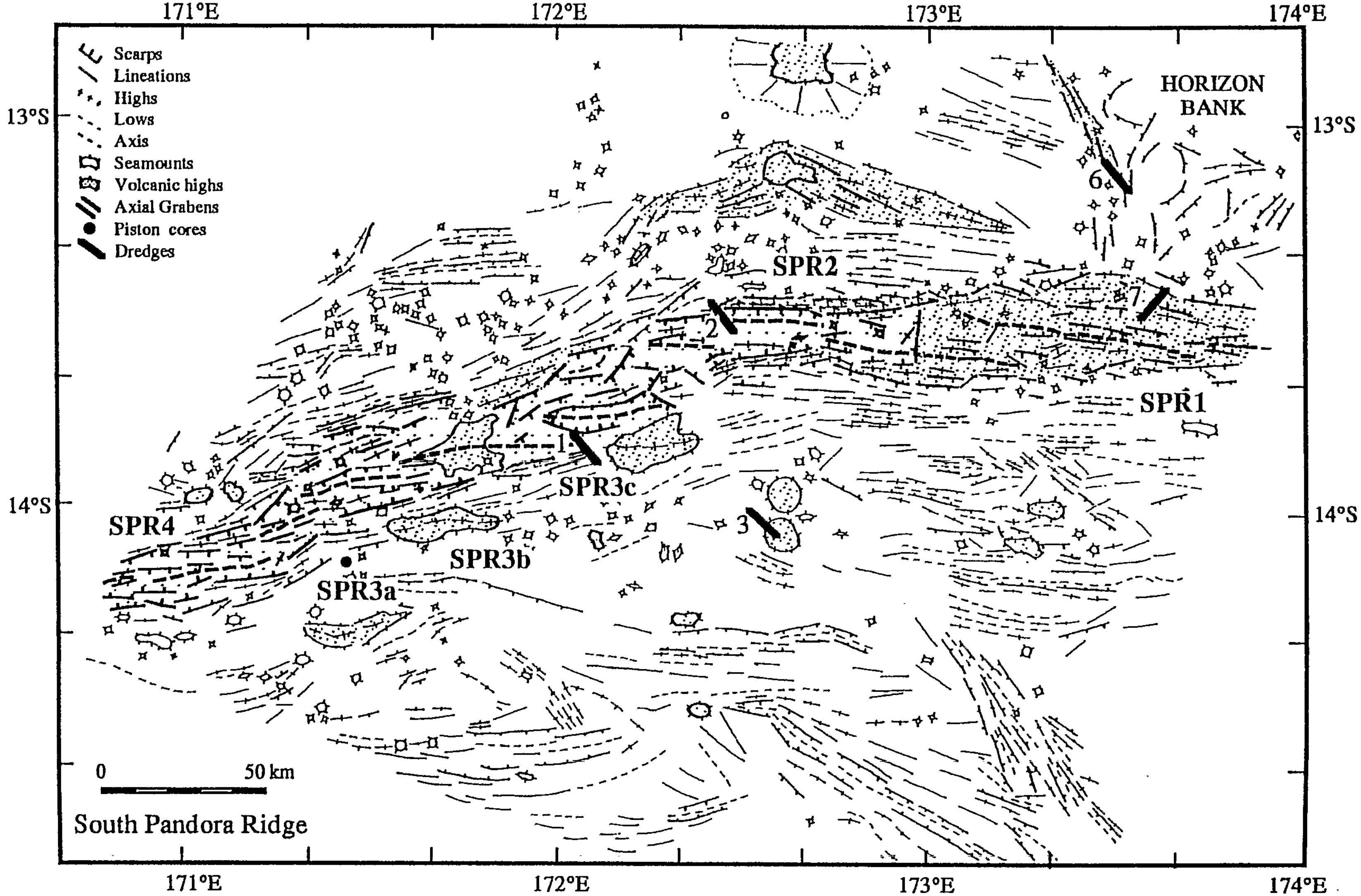

Figure 5. Detailed structural sketch of the South Pandora Ridge.

it probably extends further west with the same orientation (globally N 65° E). It shows a complex axial valley bounded by discontinuous lateral ridges trending N 75° E, N 90° E and N 105° E. The faults bounding most of the internal structures are oriented N 90° E.

In short, the five identified first-order segments, 100 km long in average, show either a 'tectonic-stage configuration' with a more or less complex deep axial valley or a 'volcanic-stage configuration' with a high, rifted volcanic massif filling up the axial domain. The broad orientation of the segments varies from N 65° E (SPR4) to N 100° E (SPR0), while the axial tectonic fabric is characterized by a constant N 90° E trend.

The axial discontinuities. Most of the discontinuities between first-order segments are associated with offsets of the axial zone and correspond to areas showing complex patterns of oblique structures, suggesting off-axis deformation (Figures 4 and 5).

At discontinuity SPR0-SPR1, the two axial volcanic highs overlap over a distance of 30–40 km, with an axis offset of 30 km. The two tips of the overlapping ridges show a typical curved pattern.

No clear overlap is observed at the discontinuity SPR2-SPR3. The apparent offset of the axis is 15–18 km. Scarps oriented N 30° E–N 40° E are abundant within the connection between the axial domains. Structures with similar orientation are observed off-axis, within a region extending 50 km northward and southward from the discontinuity. This indicates that the junction is not a transform fault, but a complex relay zone, where diffuse transfer of extensional motion occurs between the segments. However, a fault zone trending N 30° E–40° E from the northern wall of segment SPR2 to the northern wall of segment SPR3, and crosscutting the ridge, produces a clear signature in the imagery mosaïc. No significant offset in bathymetric contours is associated with this fault.

Discontinuity SPR3-SPR4 exhibits tectonic features trending roughly E–W west of 171° E and swinging gradually northward to trend N 30° E–40° E east of 171°20′ E.

3.1.2. *Geometry and structure of the Tripartite Ridge active axis, and the junction with the Rotuma Ridge*

A 100% bathymetric coverage was obtained in the western part of the TR, from 173° 40′ E to 175° 30′ E, in the region corresponding to the junction with the Rotuma Ridge (Plate A, Figure 4). The N 70° E trending Rotuma Ridge abuts against the TR at this junction, characterized by a huge volcanic high shallowing to less than 450 m (Figure 6).

The Tripartite Ridge. The TR extends along 180 km, from 174°30′ E to 177°30′ E. The general trend is N 110° E. The axial domain consists of a succession of slightly curved highs and lows, defining sigmoidal shapes. The transverse morphology of the Tripartite Ridge largely changes from profile to profile, showing either a large volcanic massif or a graben (line NF-43, Figure 9). The width of the zone showing a N 110° E ridge-parallel fabric narrows from 70 km to only a few kilometers from west to east (Figure 9, lines NF-43 and NF-44). This zone is devoid of sedimentary cover. The active ridge can no longer be identified on line NF45 along which only a very narrow graben and a half-dome are observed. These observations suggest that the Tripartite Ridge is a very young feature propagating into an older oceanic domain affected by normal faulting.

A very thin sedimentary cover (0.1 sec maximum) is observed in the area located south of the ridge. Tilted blocks dip toward the ridge and are bounded by southward facing normal faults (Figure 9, line NF-43).

Three main segments showing an axial volcanic high have been identified along the active axis of the TR (Figure 6). These segments follow a similar trend and are not affected by clear offsets, thus not allowing a clear characterization of the discontinuities between segments.

Segment TR1 is 120 km long and trends N 105° E. From east to west the axis is divided into three sub-segments, successively a graben (TR1a), a volcanic high (TR1b), and another graben (TR1c) (Figure 6). The whole segment is bounded by two lateral ridges. The TR1a graben itself is composed of three small "en echelon" grabens, trending N 110° E and separated by N 155° E transverse offsets. The TR1b sub-segment is composed of an important high (shallower than 1400 m) centered on 176°53′ E which forks at 176°46′ E into two elongated ridges.

The junction between TR1 and TR2 occurs at 176°30′ E, where the eastern tip of the TR2a graben curves towards the western TR1c graben.

Segment TR2, 70 km long, is composed of the Cakabau Seamount and a graben located on its eastern edge. The general trend of the structures is N 110° E. The eastern graben (TR2a) presents a curved shape. The Cakabau Seamount (TR2b) is a very shallow volcano centered on 175°55′ E.

Segment TR3 also consists of 2 axial grabens (TR3a and TR3c) interrupted by a central volcanic massif (TR3b). The TR3a graben itself consists of two parallel troughs. The TR3b sub-segment represents the junction between the Tripartite and Rotuma ridges. The TR3 segment ends in a curved graben (TR3c), which narrows westwards.

The South Pandora Ridge–Tripartite Ridge Junction. At 174°40′ E, a major discontinuity, offsetting the axis by 35 km, marks the junction between the TR and SPR spreading systems (Figure 6). This structure resembles a large Overlapping Spreading Center (OSC) and is composed of two overlapping curved grabens, the TR3c graben to the north and the tip of segment SPR to the south. The seafloor between the two arms of the junction shows a N 140° E fabric. This feature shows close similarities with the pattern observed west of the Fiji Islands (West Fiji Rift, Figure 2) where the spreading axis consists of two overlapping active grabens probably representing a propagating rift and a failed rift respectively (Huchon *et al.*, 1994; Auzende *et al.*, 1994).

3.2. Geophysical results

3.2.1. *Magnetics*

During the NOFI cruise, the magnetic field was almost continuously recorded by two instruments, a standard towed proton-precession magnetometer and the recently developed shipboard three-component magnetometer (Isezaki, 1986).

The three-component data are expected to provide a measure of the two/three dimensionality of the anomaly source bodies, and (in the case of two-dimensional structures) an estimate of their direction. They also represent a mean to approach the location and amplitude of the magnetization contrasts (Seama *et al.*, 1993; Korenaga, 1995), in addition to the analytic signal determination (Nabighian, 1972; Roest *et al.*, 1992) and to the technique of inversion in presence of topography (Parker and Huestis, 1974) applied to the scalar anomaly profiles. Such processes are currently being applied to the data and the results will be presented elsewhere. In this paper, we only show the scalar magnetic anomaly data.

Scalar magnetic anomalies can be easily correlated among profiles navigated about 15 km apart on the South Pandora Ridge (Figure 10). They define lineations which mimic the structures revealed by the quasi-continuous bathymetric grid. Directions of the SPR segments are clearly expressed, and the terminations of these segments are marked by interruptions in the magnetic lineations (see for instance SPR0-SPR1 and SPR3-SPR4 on Figure 11). Spacing of the various recognized anomalies does not vary significantly along the SPR, suggesting a fairly constant spreading rate. Despite a poorer data coverage, the Tripartite Ridge is also associated to correlatable magnetic anomalies. The lineations associated to the TR get closer to the east on both flanks, suggesting a spreading rate decreasing eastward. The same anomaly observed off-axis on the northern ridge flank can apparently be traced up to the TR eastern tip. The Rotuma Ridge, which has been only surveyed by three profiles, displays a rather consistent magnetic signature on those profiles, with a relatively narrow and weak positive anomaly flanked by two negatives (Figure 11).

The lineations reproduce structural details down to a scale of a few tenths of kilometers with a good accuracy, suggesting that in areas where detailed basement topography is not available (thick sedimentary cover, aeromagnetic data, ...) dense magnetic surveys provide a trustable substitute for structural analysis (e.g. Dyment, 1993). For instance, magnetic lineations clearly show the change in structural trend also observed on the bathymetry between 172°40′ E–173°25′ E, 12°50′ S–13°30′ S. Many other examples may be found from the comparison of Plate A and Figure 10, including sigmoidal patterns at the junction of segments SPR0 and TR3, curved fabrics on the southern flank of segment SPR0, at the western end of segment SPR2, on both flanks of segment SPR3, and at the eastern end of segment SPR4. A last example can be found along a E–W scarp located at 14°18′ S and between 173° E and 174° E, which defines the limit between the roughly E–W fabric associated to the SPR and a N 160° E fabric associated to the northernmost part of the Central Spreading Ridge. This scarp is marked by a continuous positive magnetic anomaly which follows its sinuosities between 173°20′ E and 173°30′ E. Magnetic lineations trend E–W to the north and N 160° E to the south of the scarp.

Due to the complexity of the seafloor spreading patterns in the NOFI cruise area, identification of magnetic anomalies on single profiles is not an easy task. Axial anomalies are associated with high reflectivity of the side-scan imagery, and are therefore the most easily recognized. Along the SPR, the axial anomalies are usually about 15 km wide, and display strong variations of amplitude. These variations may be partly attributed to the important variations of axial bathymetry. However, it is likely that additional variations of the source parameters (extrusive basalt thickness? magnetization?) should also be invoked (see Dyment and Arkani-Hamed, 1995, for a review of possible processes). Data on the Tripartite and Rotuma Ridges are more difficult to interpret. In both cases, axial anomalies may be inferred from the available profiles, but no sequence of older conjugate anomalies has been convincingly recognized on the flanks. On the contrary, the SPR displays clear conjugate sequences of anomalies which have been interpreted from relatively undisturbed (according to the bathymetric grid) profiles.

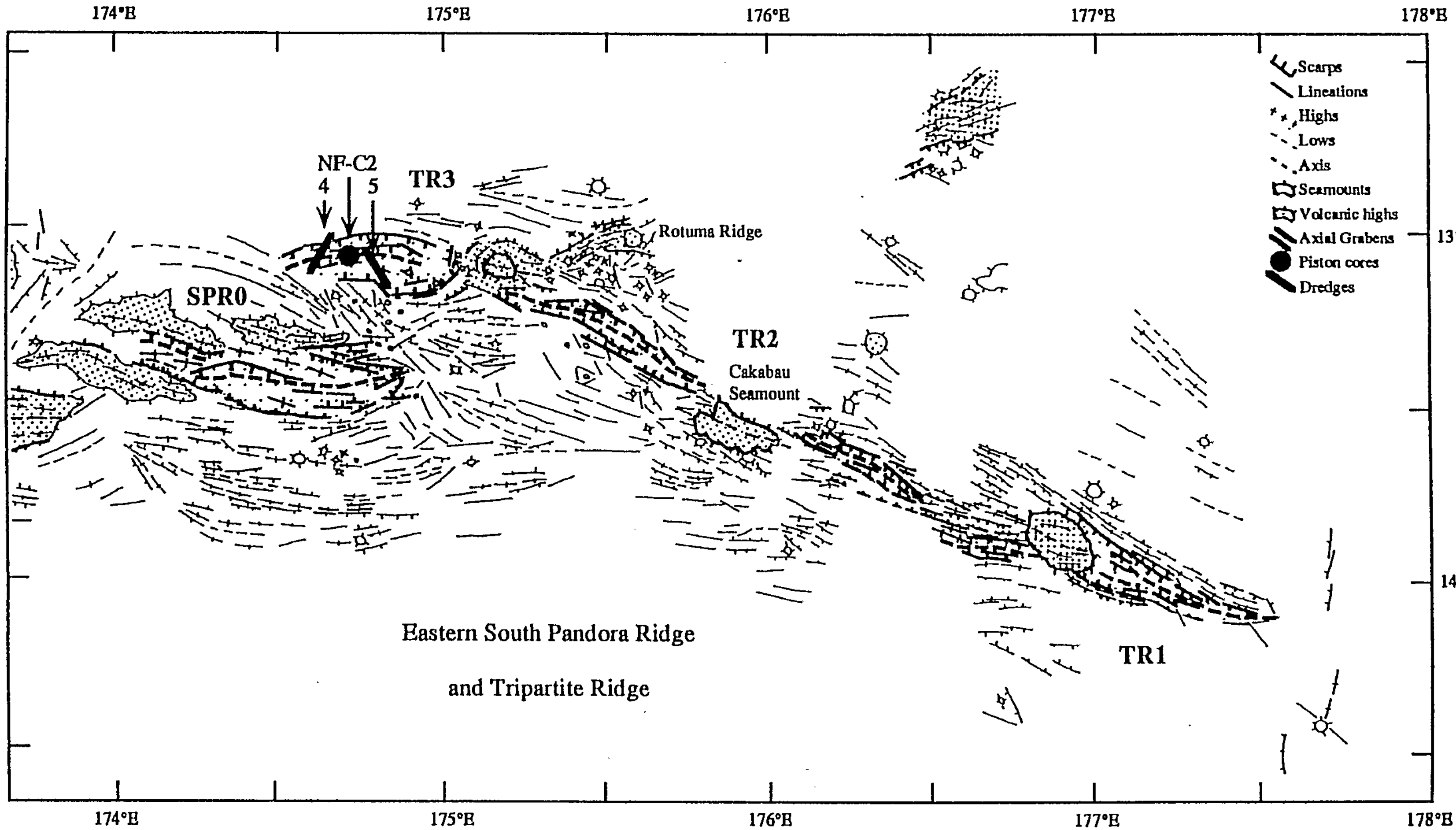

Figure 6. Detailed structural sketch of the Tripartite Ridge.

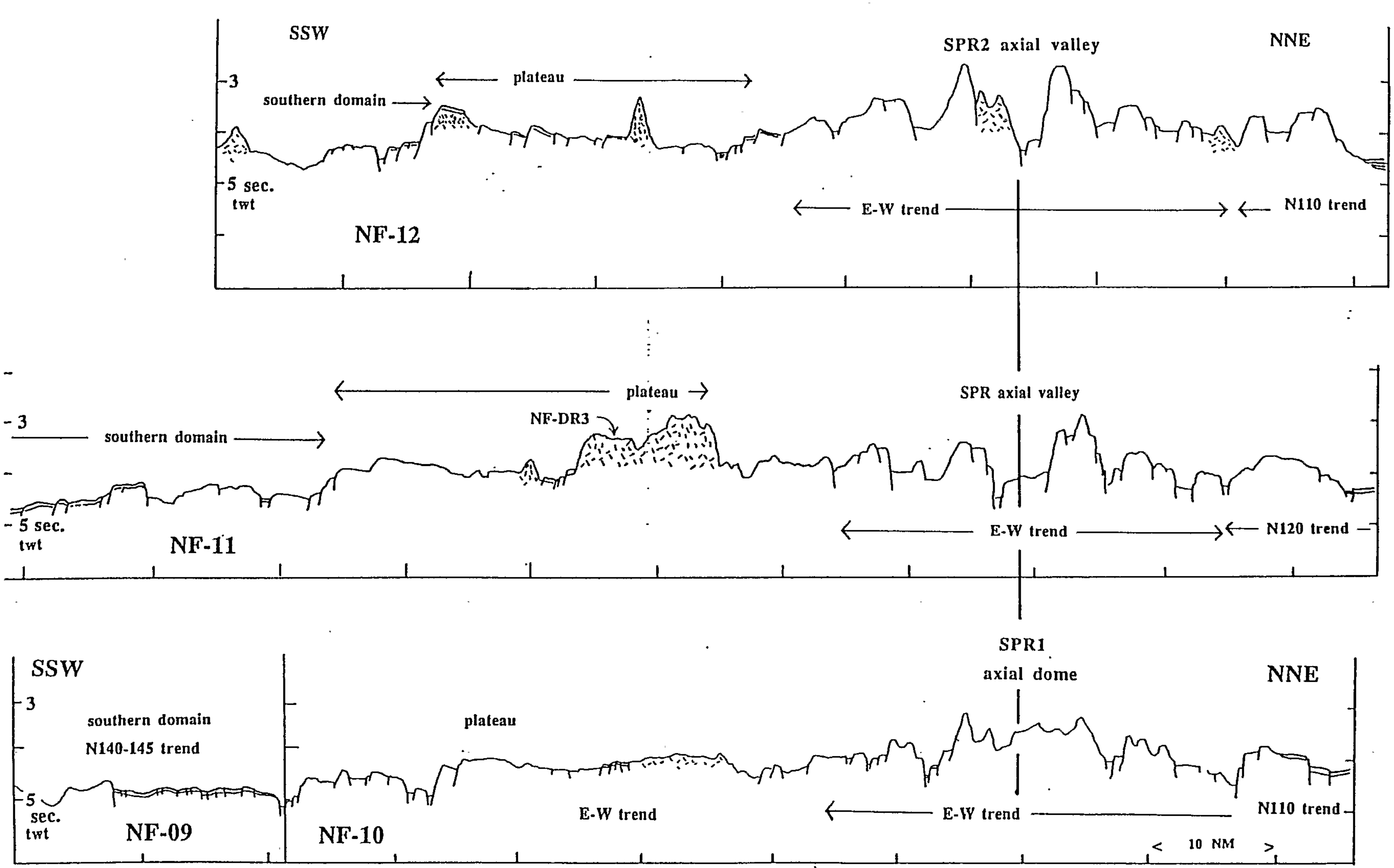

Figure 7. Selected line drawings of 6-channel reflection seismic lines across segment SPR1 and SPR2 of the South Pandora Ridge.

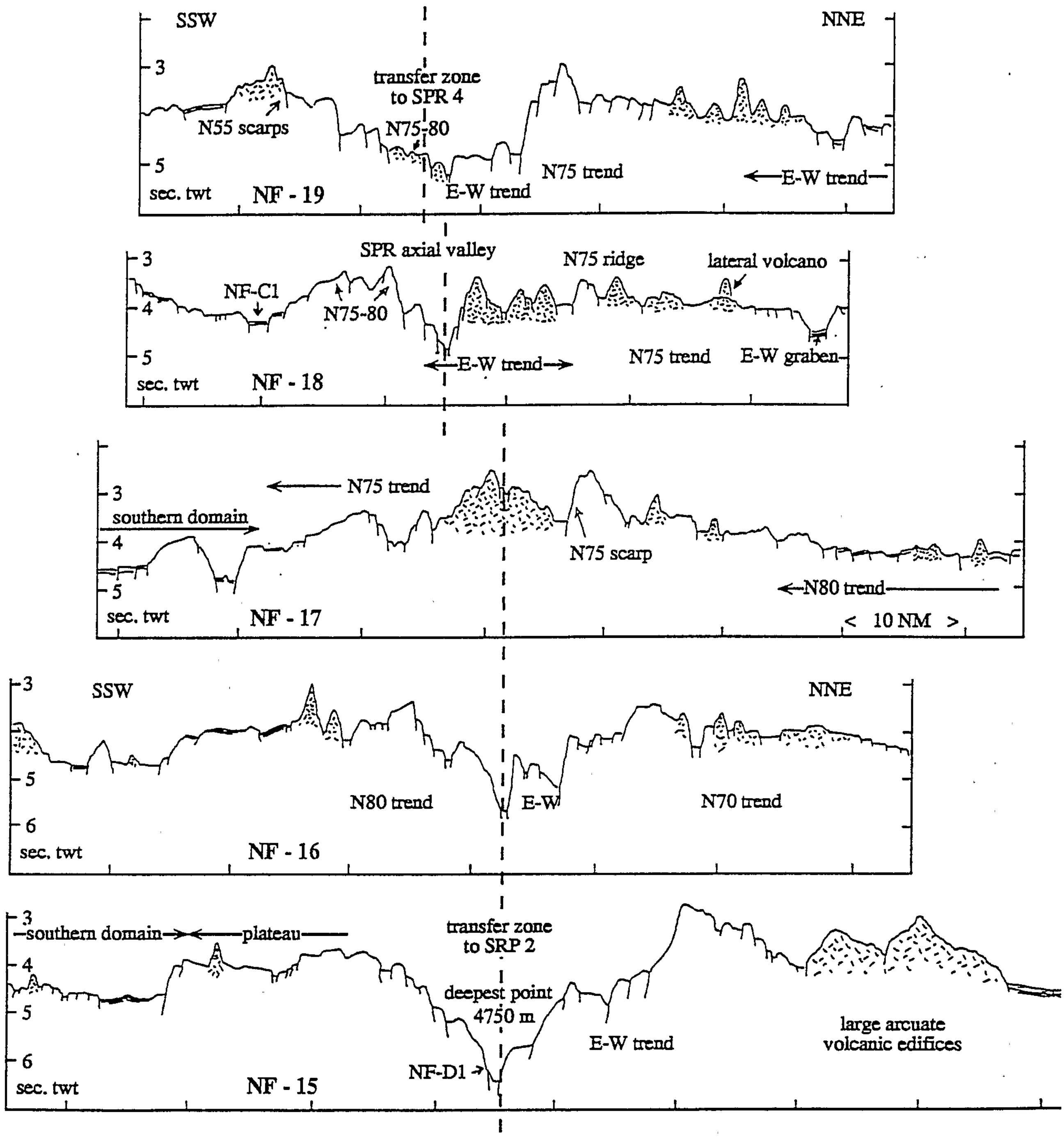

Figure 8. Selected line drawings of 6-channel reflection seismic lines across segment SPR3 of the South Pandora Ridge. Dotted line represents the location of the active axis.

Figure 11 shows two profiles north and south of the SPR, cutting accross roughly conjugate areas (the profiles are oblique with respect to the SPR, so conjugate areas are surveyed by different profiles). These profiles display anomalies 1 to 3A on both flanks, as shown by comparison with a simple magnetic model (Figure 12), and therefore suggest that the SPR exists since at least 7 Ma. Despite local change of lineation direction accomodated by spreading assymetry and other complex spreading patterns, these anomalies can

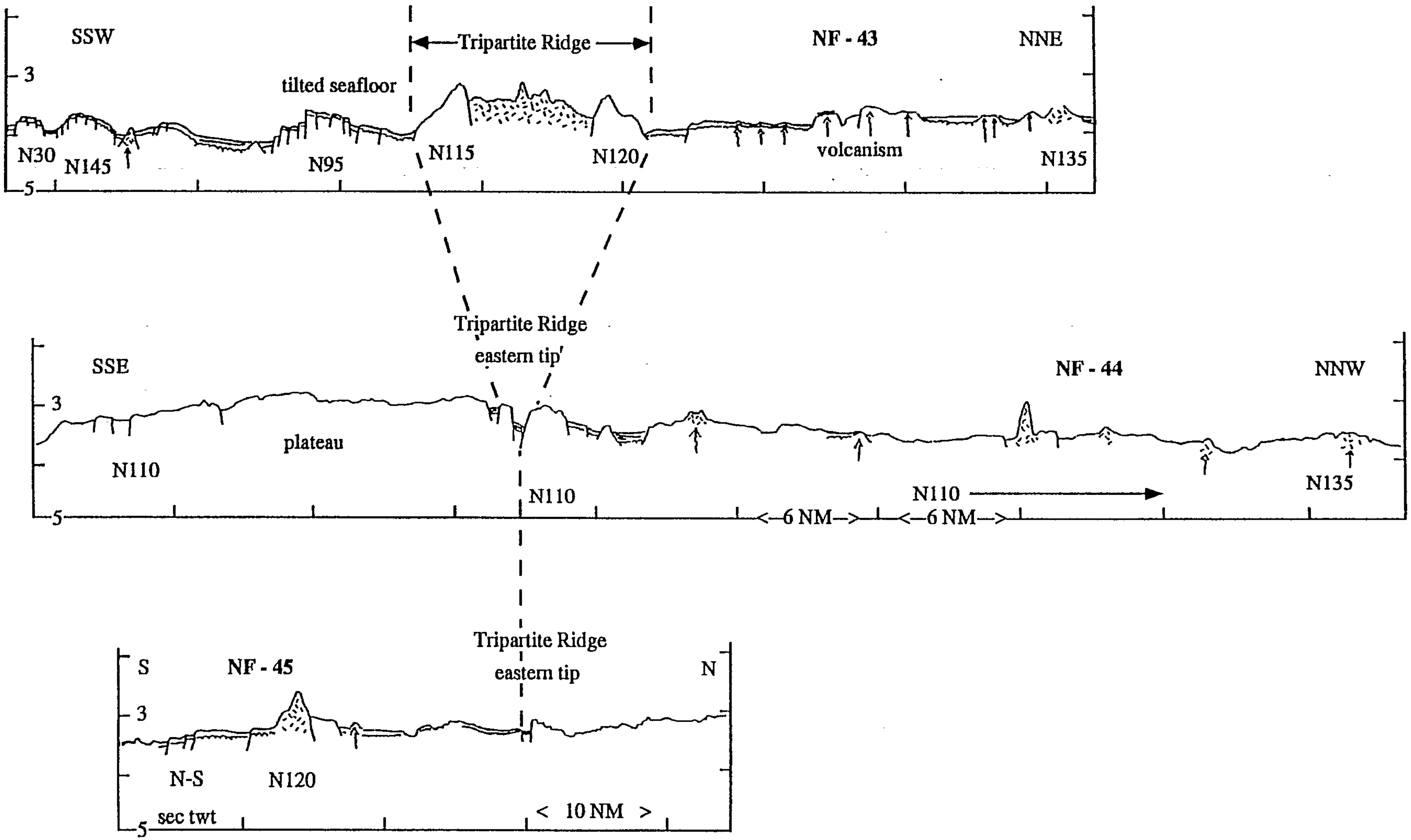

Figure 9. Selected line drawings of 6-channel reflection seismic lines across segment TR1 of the Tripartite Ridge. Dotted line represents the limits of the recent crust emplaced at the spreading axis.

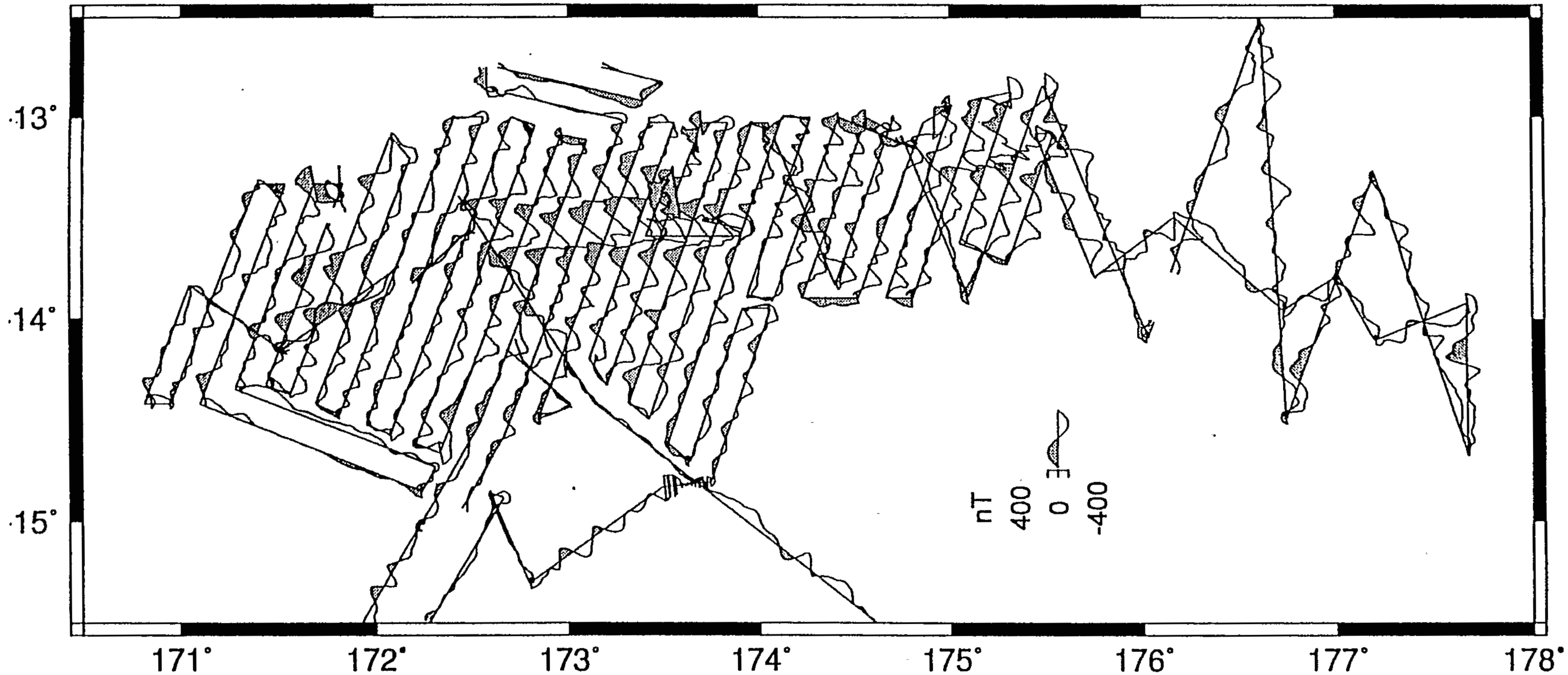

Figure 10. Scalar magnetic anomaly projected orthogonally to the ship's tracks. Positive anomalies are shaded.

be followed along segments SPR1 and SPR2. This interpretation implies an average half spreading rate of about 8 km/m.y., varying locally as a result of oblique and asymmetric spreading and slightly decreasing during the period considered. The scarp separating E–W and N 160° E fabrics corresponds to chron 3Ar (r for reversed, i.e. the reversed period immediately before chron 3A), dated 7.2 Ma. This scarp may have been created by the initiation of spreading along this SPR segment at 7.2 Ma within older oceanic lithosphere created at an older spreading axis. To the west, along profile NF31 (Figure 3), anomalies 4 to 5 may be tentatively identified (8–10 Ma). Their northern conjugates have not been recognized and may lie north of the surveyed area. These anomalies are located on oceanic lithosphere which display E–W fabric, west and north of two grabens which are supposed to represent the northernmost expression of the N 160° E branch of the Central Spreading System. Immediately south of anomaly 5 (younger part), the E–W fabric is interrupted and gives place to a varying N 110° E to N 150° fabric. Anomalies on the northern flank are partially hidden by seamounts at 172°40′ E and 173°40′ E, and the survey does not extend as far north of the SPR as it does to the south, making difficult the search for anomalies older than 3A.

Due to their lower amplitudes, anomalies are more difficult to interpret on segments SPR3 and SPR4. Preliminary interpretation of anomalies along profiles NF17 and NF18 suggests that conjugate anomalies 1 to 3A exist in segment SPR3, with a systematic spreading assymetry benefiting to the northern flank. Only anomalies 1 and 2 are identified on the surveyed part of segment SPR4. Anomalies 1 to 3A (3 on the southern flank) are also identified on segment SPR0, although in a less reliable way due to complex curved patterns, limited survey extension, and lower amplitude of the anomalies. Anomalies 1 to 3 and 1-2 are finally observed on the southern and northern flanks of segment TR3, respectively.

3.2.2. Gravity

Gravity data were almost continuously recorded while the ship was underway during the NOFI cruise, except when the ship approached dredging or coring stations. The cross-over errors over the SPR box, between the NNE-SSW trending profiles NF-10 to NF-19, NF-22, -23, -24 and the "wiggly" composite profile NF-25 to NF-30 (see Figure 3 for the location of these profiles) are 1 ± 0.5 mgal. This shows that the gravity sensor underwent little drift during the NOFI cruise, as was further confirmed by harbor tie-ins performed in Noumea at the beginning and end of the cruise.

The gravity data were used to contour a free-air anomaly map over the South Pandora Ridge (Figure 13). The wider spacing of the ship's tracks over the Tripartite Ridge precludes a straightforward interpretation of a free-air anomaly map contoured solely from ship's data. An interpretation of gravity data along the ship's tracks by spectral analysis methods will appear in Matsumoto *et al.* (in press).

As expected, the distribution of free-air anomalies is strongly correlated with the main topographic features of the South Pandora Ridge, as revealed by the bathymetric and sonar imagery surveys.

The four main segments and sub-segments identified along the South Pandora Ridge, produce a clear signature on the free-air anomaly map:

- the eastern segment SPR1, a large high volcanic province, produces a broad positive anomaly. The Horizon Bank, where shallow depths result in free-air anomalies over +120 mgal, appears clearly connected to segment SPR1, as shown by the closure of the gravity contours around these two features.
- transition between segment SPR1 and segment SPR2 appears relatively graduate on the free-air anomaly map, segment SPR2a producing a negative anomaly. The other lows, termed SPR2b and SPR2c, produce larger negative anomalies.
- the three sub-segments SPR3a to SPR3c are apparent on the free-air anomaly map. Transitions between these sub-segments are extremely sharp. Segment SPR3a, which includes the "Nofi deep", in which the deepest soundings of the NOFI survey have been observed, corresponds to a negative anomaly, whose amplitude, however, does not exceed the ones observed over segments SPR2b and SPR2c.
- the transition towards segment SPR4 appears broad and marked by a small-amplitude negative anomaly. Segment SPR4 itself produces also a small negative anomaly.

The interpretation of mantle Bouguer anomaly maps is presently underway and should bring information both on small-scale crustal thickness variations along the SPR and on larger scale temperature structure of the area.

A few off-ridge features also stand out on the free-air anomaly map. The large arcuate volcanic ridge located north of segment SPR2 is underlined by the bending of the gravity contours. Even more apparent are the active tip of the N 160 branch of the Central Spreading Ridge and the N 140 trending complex low which extends from the N 160 branch of the Central Spreading Ridge to the SPR3-SPR4 relay zone. This

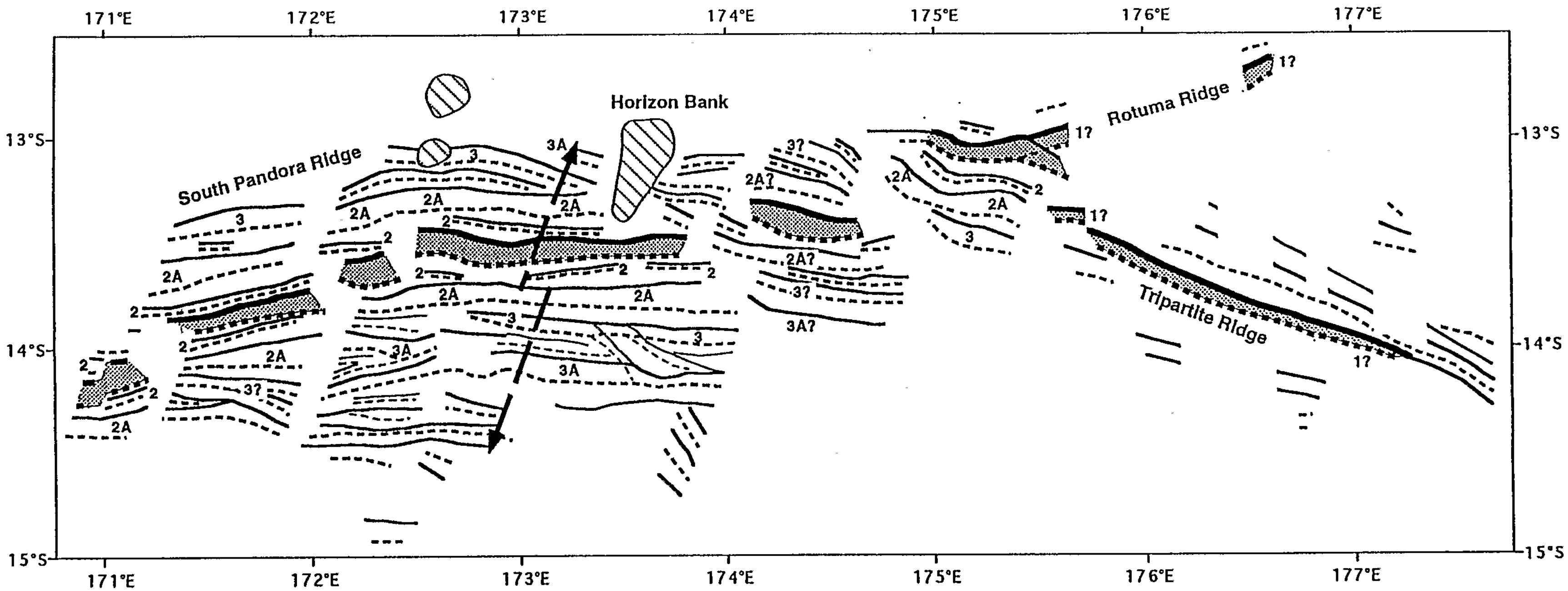

Figure 11. Magnetic lineations as interpreted from Figure 9. Solid lines : positive anomalies, dashed lines: negative anomalies. Bold dashed arrows indicate the location of the composite profile modelled on Figure 11.

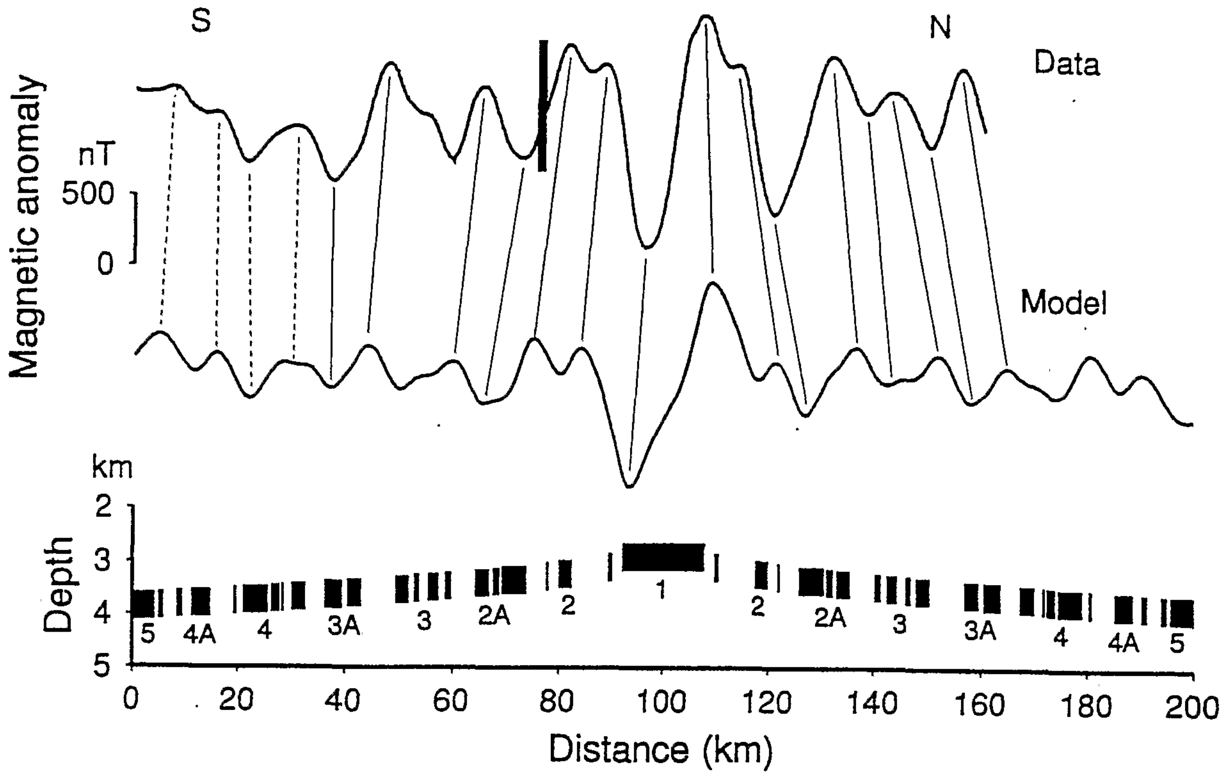

Figure 12. Identification of magnetic anomalies along a composite profile at longitude 173° E projected in the N–S (spreading) direction. The bold line locates the limit between the two ship's tracks (see caption of *figure 11*). Model is computed at 14° S and 173° E for an E–W trending ridge with (half) spreading rate of 10 km/m.y.

last feature appears as an important link between the two spreading systems.

4. Conclusions

The NOFI cruise provides new insights on the geometry and evolution of the spreading axes in the Northern North Fiji Basin. The South Pandora and Tripartite spreading centres exhibit morphometric characteristics of oceanic ridges and display typical geophysical signatures of active spreading systems. The axial part of the spreading ridge shows a discontinuous pattern, with segment lengths ranging from 80 to 100 km. No clear transform faults are observed, whereas complex relay zones separate the first-order segments. As clearly shown on the acoustic imagery map, the active tectonic and volcanic zone corresponds to high-reflectivity terranes which form an almost continuous, E–W oriented broad arch. The average width of the active domain is 20 km and corresponds to either bathymetric highs or deep elongated grabens. The 3000 m to 4800 m deep grabens show the typical morphology of slow spreading axes. Volcanic constructions may obstruct totally the central valley. Dredges performed at several places within the axial domain confirm that basaltic lavas have been emplaced very recently at the spreading center. The main segments and sub-segments identified along the South Pandora Ridge produce a clear signature on the free-air gravity anomaly map. Well-organized magnetic lineations parallel or slightly oblique to the active axis are observed along both the South Pandora Ridge and the Tripartite Ridge. Our preliminary interpretation of magnetic anomalies along selected profiles suggests that conjugate anomalies 1 to 3A exist in segment SPR3 indicating seafloor spreading at a very low rate since at least 7.2 My.

Finally, three main results relevant to the geodynamic evolution of the North Fiji Basin can be outlined from the preliminary analysis of the new detailed data set obtained from this back-arc spreading system:

1. Relatively old crust (7.2 Ma, and probably older) is present in the Northern NFB, confirming previous results derived from the interpretation of widely spaced geophysical surveys over this area (Pelletier *et al.*, 1993a).

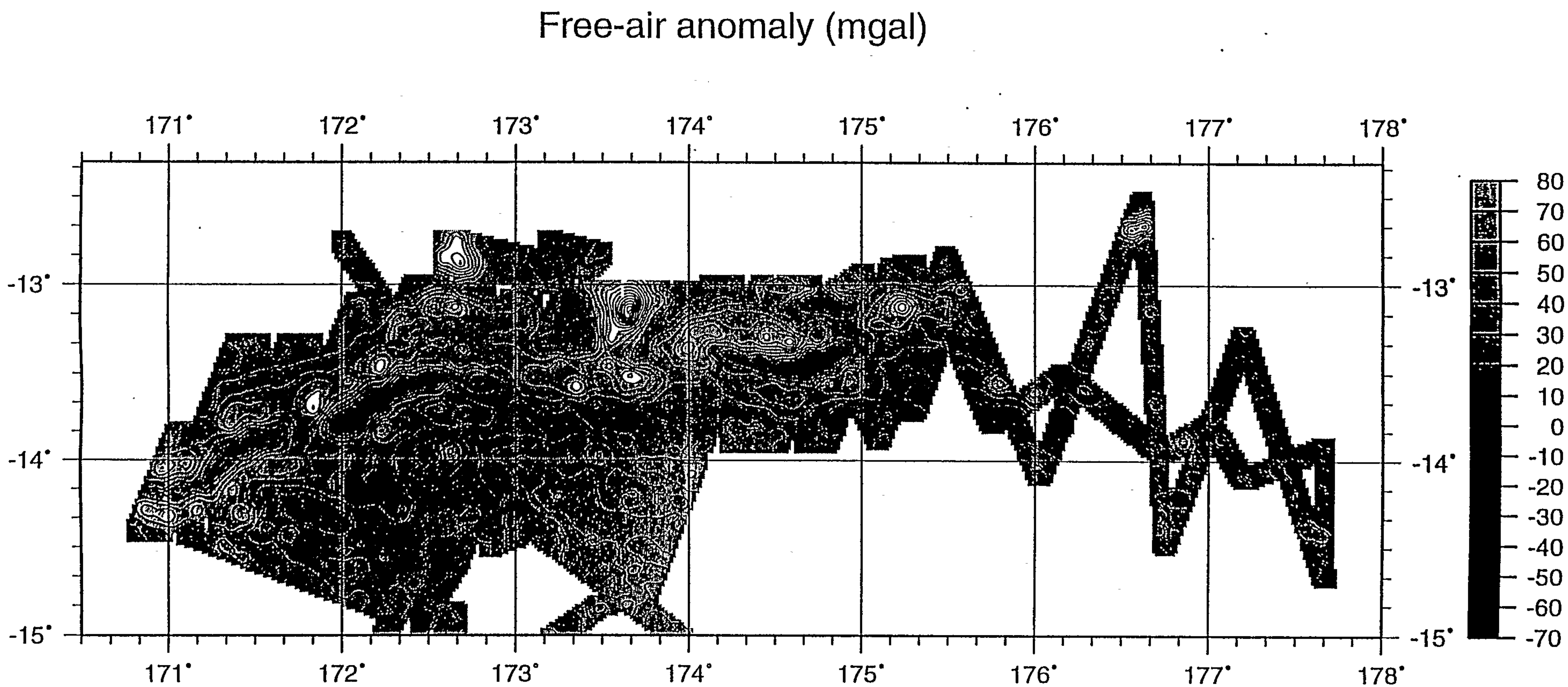

Figure 13. Free-air gravity anomaly map over the South Pandora Ridge contoured from along-track data from the NOFI cruise.

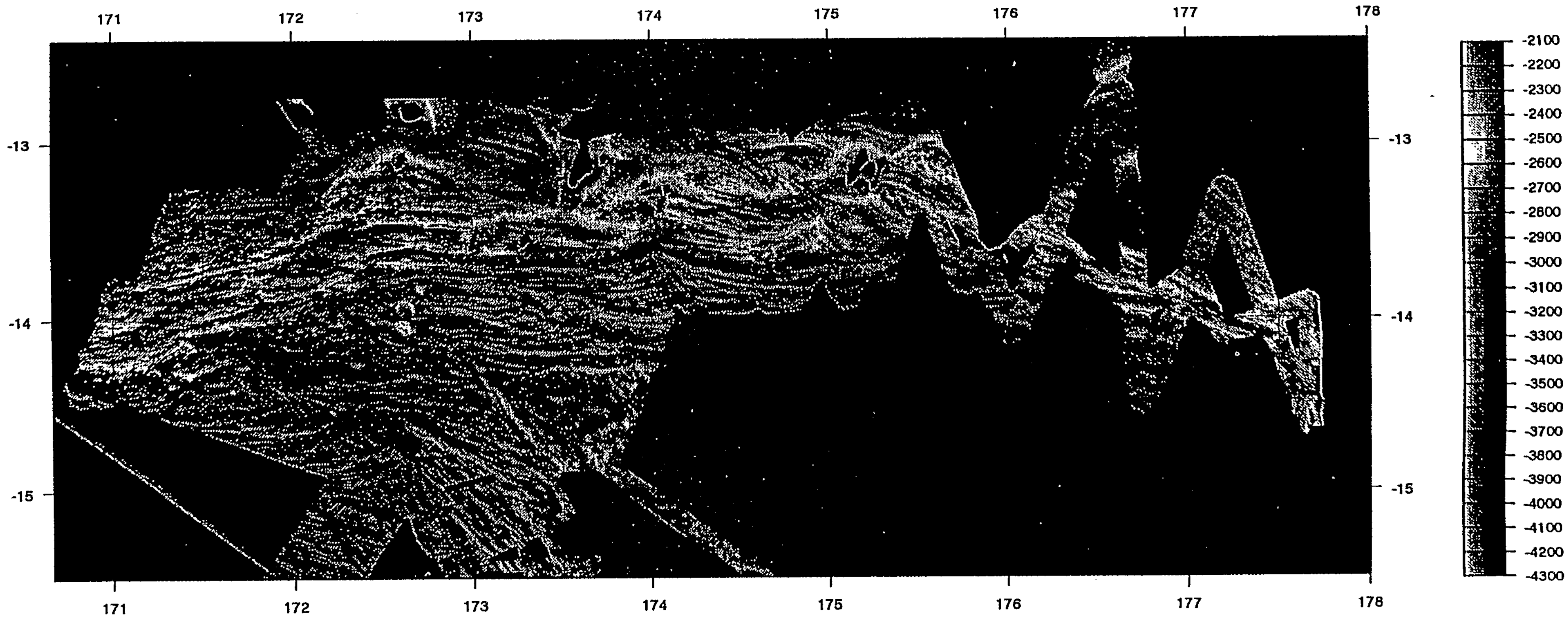

Plate A: Bathymetry from the NOFI survey (computed with the help of TRISMUS software). Illumination is from the North.

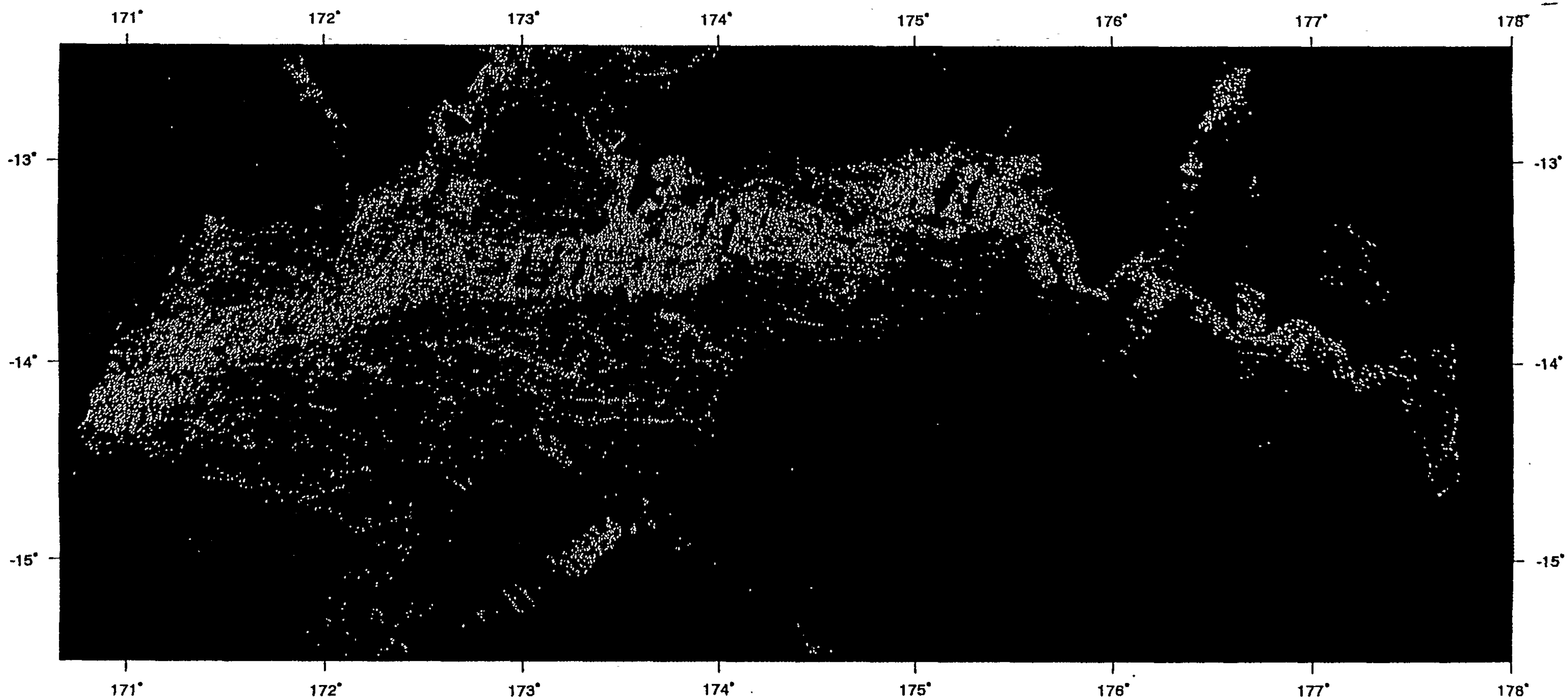

Plate B: Multi-beam acoustic image of the South Pandora and Tripartite ridges. Red shades correspond to high-reflectivity areas.

2. Oceanic spreading processes are occurring almost continuously since at least 7 Ma along the South Pandora Ridge spreading system, with a relatively stable geometry as revealed by the well-organized, parallel pattern of magnetic lineations at a regional scale. However, at a smaller scale, many examples of sigmoidal patterns and curved fabrics indicate local complexity in the geometry of the spreading axis. Similar changes in the geometry of the Central Spreading Ridge, located further south, including recent reorganizations at 3 Ma and 1.5 Ma have been reported by Auzende *et al.* (1995). As revealed by a complex seafloor fabric in the junction region between the SPR and the CSR, it is likely that interactions between these orthogonal spreading systems occurred repeatedly in relation with these major changes.
3. The eastern part of the surveyed area, including the Rotuma and Tripartite ridges, is the most active region in terms of propagations and reorganizations of the spreading centers. These features collectively demonstrate that the northeastern part of the North Fiji Basin is undergoing active deformation. A recent SOPACMAPS survey of the Vitiaz Trench north of the Tripartite and Rotuma ridges has also demonstrated that active deformation exists along this presumed "fossil" boundary (Pelletier *et al.*, 1994).

Acknowledgements

We thank the captain R. Derouet and the *GENAVIR* crew of the R/V *L 'Atalante* for their efforts to ensure collection of high quality data. Trismus and Imagem softwares used to process bathymetry and imagery data were developed by *IFREMER*. Most of the figures presented in this paper were drawn with the help of GMT software (Wessel and Smith, 1991). Financial support was provided by CNRS/INSU through "Soutien aux campagnes à la mer" and "Géosciences Marines". Bryan Taylor, Jean-Marie Auzende and an anonymous reviewer made useful comments which greatly improved the manuscript.

References

Auzende, J. M., Pelletier, B., and Eissen, J. P., 1995. The North Fiji Basin: Geology, Structure and Geodynamic Evolution, in Backarc Basins: Tectonics and Magmatism. B. Taylor (ed.) Plenum Press, New York.

Auzende, J. M., Pelletier, B., and Lafoy, Y., 1994, Twin Active Spreading Ridges in the North Fiji Basin. *Geology*, **22** 63–66.

Auzende, J. M., Eissen J. P., Lafoy Y., Gente P., and Charlou J. L., 1988a, Seafloor Spreading in the North Fiji Basin (Southwest Pacific), *Tectonophysics* **46**, 317–351.

Auzende, J. M., Lafoy Y., and Marsset B., 1988b, Recent geodynamic evolution of the North Fiji Basin (SW Pacific), *Geology* 16, 925–929.

Chase C. G., 1971, Tectonic History of the Fiji Plateau, *Geol. Soc. Am. Bull.* **82**, 3087–3110.

Cherkis, N. Z., 1980, Aeromagnetic Investigations and Sea Floor Spreading History in the Lau Basin and Northern Fiji Plateau, in W. J. Clark (ed.), "Symposium on Petroleum Potential in Island Arcs, Small Basins, Submerged Margins and Related Areas", *UN ESCAP, CCOP/SOPAC Techn. Bull.* 3, 37–45.

de Alteris, G., Ruellan, E., Auzende, J. M., Ondréas, H., Bendel, V., Gracia-Mont, E., Lagabrielle, Y., Huchon, P., and Tanahashi, M., 1993, Propagating Rifts in the North Fiji Basin (Southwest Pacific), *Geology* 17, 583–586.

Dyment, J., 1993, Evolution of the Indian Ocean Triple Junction Between 65 and 49 Ma, Anomalies 28 to 21), *J. Geophys. Res.* **98**, 13,863–13,877.

Dyment, J. and Arkani-Hamed, J., 1995, Spreading Rate Dependent Magnetization of the Oceanic Lithosphere Inferred from the Anomalous Skewness of Marine Magnetic Anomalies, *Geophys. J. Int.*, **121**, 789–804.

Eguchi, T., 1984, Seismotectonics of the Fiji Plateau and Lau Basin, *Tectonophysics* **102**, 17–32.

Fox, P. J., Grindlay, N. R., and Macdonald, K. C., 1991, The Mid-Atlantic Ridge (31° S-34°30 S): Temporal and Spatial Variations of Accretionary Processes, *Mar. Geophys. Res.* 13, 1–20.

Gente, P., 1987, Etude morphostructurale comparative des dorsales océaniques à taux d'expansion variés. Schéma d'évolution morphologique de l'axe des dorsales: liaisons avec l'hydrothermalisme. *Thèse Doc. Univ. Bretagne Occidentale*, Brest, 371 p.

Gracia, E., Ondréas, H., Bendel, V., and STARMER group, 1994, Multi-scale Morphologic Variability of the North Fiji Basin Ridge (Southwest Pacific). *Marine Geology* **116**, 133–151.

Gracia, E., Tisseau, C., Maia, M., Tonnerre, T., Auzende, J. M., and Lagabrielle, Y., 1996, Variability of the Axial Morphology and Gravity Structure of the Central Spreading Ridge (North Fiji Basin): Application of a Non-Steady State Thermal Model. *Marine Geophys. Res.*, **18**, 249–273 (this issue).

Hamburger, M. W. and Isacks, B. L., 1988, Diffuse Back-Arc Deformation in the Southwestern Pacific, *Nature* 332, 599–604.

Hamburger, M. W. and Isacks, B. L., 1994, Shallow Seismicity of the North Fiji Basin, in L. W. Kroenke and J. V. Eade (eds.), "Geological Investigations of the North Fiji Basin", *Circum-Pacific Council for Energy and Mineral Resources, Earth Science Series.*

Huchon, P., Gracia, E., Ruellan, E., Joshima, M., and Auzende, J. M., 1994, Kinematics of Active Spreading in the Central North Fiji Basin (SW Pacific). *Marine Geology* **116**, 69–88.

Isezaki, N., 1986, A New Shipboard Three-Component Magnetometer, *Geophysics* **51**, 1992–1998.

Jarvis, P., Hughes-Clarke, J., Tanahashi, M., Kroenke, L., and Tiffin D., 1994, The Structure of the Fiji Fracture Zone and its Bearing on the Developement of the North Fiji Basin, in the North Fiji Basin (SW Pacific), *Marine Geology* **116**, 57–68.

Jarvis, P., Kroenke, L., Price, R., and Maillet, P., 1993, GLORIA Imagery of Sea Floor Structures in the Northern North Fiji Basin, *Geo-Marine Letters* 13, 90–97.

Kellog, J. N. and Kansakar, D. R., 1994, Gravity Field of the North Fiji Basin, in L. W. Kroenke and J. V. Eade (eds.), "Basin Formation, Ridge Crest Processes and Metalogenesis in the North Fiji Basin", *Circum Pacific Council for Energy and Mineral Resources, Earth Science Series* **12**, 41–49.

Korenaga, J., 1995, Comprehensive Analysis of Marine Magnetic Vector Anomalies, *J. Geophys. Res.* **100**, 365–378.

Kroenke, L. W. and Shipboard Party, 1987, CCOP/SOPAC Cruise Report: North Fiji Basin Expedition. R.V. Moana Wave Cruise MW87-01, 37 p.

Kroenke, L. W., Price, R. C., and Jarvis, P. A., 1991, North Fiji Basin, 1:250,000, Pacific Seafloor Atlas, Hawaii Institute of Geophysics, Honolulu, HI, Sheets n° 10 to 17.

Kroenke, L. W., Eade, J. V., and Scientific Party, 1994, Overview and Principal Results of the Second Leg of the First Joint CCOP/SOPAC-Tripartite Cruise of the R/V Kana Keoki: North Fiji Basin survey (KK820316 Leg 03), in L. W. Kroenke and J. V. Eade (eds.), "Basin Formation, Ridge Crest Processes and Metalogenesis in the North Fiji Basin" *Circum Pacific Council for Energy and Mineral Resources, Earth Science Series* **12**, 1–11.

Lapouille, A., 1986, Present-Day Opening of the Northwestern Part of the North Fiji Basin (Soutwest Pacific), South Pacific Marine Geol. Notes, Tech. Sec., CCOP/SOPAC, Suva, 3, 2, 23–27.

Larue, B. M., Pontoise, B., Malahoff, A., Lapouille, A., and Latham, G. V., 1982, Bassins Marginaux Actifs du Sud-Ouest Pacifique: plateau Nord-Fidjien, bassin de Lau, in "Contribution à l'étude géodynamique du Sud-Ouest Pacifique". Equipe de Géologie-Géophysique du Centre ORSTOM de Nouméa. *Travaux et Documents de l'ORSTOM* **147**, 363–406.

Louat, R. and Pelletier, B., 1989, Seismotectonics and Present-Day Relative Plate Motion in the New Hebrides Arc-North Fiji Basin Region, *Tectonophysics* **167**, 41–55.

Macdonald, K. C., 1986, The Crest of the Mid-Atlantic Ridge: Models for Crustal Generation and Tectonics, in: Vogt, P. R. and Tucholke, B. E. (eds.), The Geology of North-America, vol. M, The Western North Atlantic Region, Geological Society of America, Boulder, Colo., 51–68.

Macdonald, K. C., Fox, P. J., Miller, S., Carbotte, S., Edwards, M. H., Eisen, M., Fornari, D. J., Perram, L., Pockalny, R., Scheirer, D., Tighe, S., Weiland, C., and Wilson, D., 1992, The East-Pacific Rise and its Flanks 8–18 N: History of Segmentation, Propagation and Spreading Direction Based on SeaMarc II and Sea Beam Studies. *Mar. Geophys. Res.* **14**, 299–344.

Malahoff, A., Hammond, S., and Feden, R., 1979, Back-Arc Spreading, Volcanism and Evolution of the Havre Trough-Lau Basin- Fiji Plateau. Hawaii Symp. Intraplate Volcanism and Submarine Volcanism, Hilo, Hawaii (1979), abstract p. 113.

Malahoff, A., Kroenke, L. W., Cherkis, N., and Brozena, J., 1994, Magnetic and Tectonic Fabric of the North Fiji and Lau Basins, in L. W. Kroenke and J. V. Eade (eds.), "Basin Formation, Ridge Crest Processes and Metalogenesis in the North Fiji Basin", *Circum Pacific Council for Energy and Mineral Resources, Earth Science Series* **12**, 49–63.

Matsumoto, M., Goslin, J., Lagabrielle, Y., Ruellan, E., and Tanahashi, M., 1996, Gravity Anomaly and Tectonics in the Northern Part of the North Fiji Basin – Preliminary Result of the 1994 NOFI Cruise under the NEW STARMER Program. *Mar. Geophys. Res.* (in press).

Nabighian, M. N., 1972, The Analytic Signal of Two-Dimensional Magnetic Bodies with Polygonal Cross-Section: Its Properties and Use for Automated Anomaly Interpretation, *Geophysics* **37**, 507–517.

Palmer, J., Sempéré, J. C., Christie, D. M., and Phipps Morgan, J., 1993, Morphology and Tectonics of the Australian-Antarctic Discordance Between 123° E and 128° E. *Mar. Geophys. Res.* **15**, 121–152.

Parker, R.L. and Huestis, S. P., 1974, The Inversion of Magnetic Anomalies in Presence of Topography, *J. Geophys. Res.* **79**, 1587–1593.

Pelletier, B., Lafoy, Y., and Missegue, F., 1993a, Morphostructure and Magnetic Fabric of the Northwestern North Fiji Basin. *Geophys. Res. Lett.* **20** (12), 1151–1154.

Pelletier, B., Missègue, F., Lafoy, Y., Mollard, L., Decourt, R., Dupont, J., Join, Y., Perrier, J., and Récy, J., 1993b, Extrémités Nord Du bassin Nord-Fidjien et des Fossés Arrière-arc des Nouvelles-Hébrides: Morphostructure et Signature Magnétique, *C.R. Acad. Sci. Paris* **316**, II, 637–644.

Pelletier, B., Auzende, J. M., and Daniel, J., 1994, Main Results of the SOPACMAPS Cruise: Mapping of the Boundary of Pacific-Australian Plates. Seafloor Mapping in the West and Southwest Pacific, Results and Applications. Lifou-Nouméa, 4–9 Nov. 1994. Abstract, p. 57.

Price, R. C. and Kroenke, L. W., 1991, Tectonics and Magma Genesis in the Northern North Fiji Basin, *Marine Geology* **98**, 241–258.

Price, R. C., Johnson, L. E., and Crawford, A. J., 1990, Basalts of the North Fiji Basin: The Generation of Back-Arc Basin Magmas by Mixing of Depleted and Enriched Mantle Sources, *Contrib. Mineral. Petrol.* **105**, 106–121.

Purdy, G. M., Sempéré, J. C., Schouten, H., Dubois, D. L., and Goldsmith, R., 1990, Bathymetry of the Mid-Atlantic Ridge, 24°–31° N: A Map Series. *Mar. Geophys. Res.* **12**, 247–252.

Roest, W. R., Arkani-Hamed, J., and Verhoef, J., 1992, The Seafloor Spreading Rate Dependence of the Anomalous Skewness of Marine Magnetic Anomalies, *Geophys. J. Int.* **109**, 653–669.

Ruellan, E., Huchon, P., Auzende, J. M., and Gracia, E., 1994, Propagating Rift and Overlapping Spreading Center in the North Fiji Basin. *Marine Geology* **11**, 37–56.

Seama, N., Nogi, Y., and Isezaki, N., A New Method for Precise Determination of the Position and Strike of Magnetic Boundaries Using Vector Data of the Geomagnetic Anomaly Field, *Geophys. J. Int.* **113**, 155–164.

Sempéré, J. C., Purdy, G. M. and Schouten, H., 1990, The Segmentation of the Mid-Atlantic Ridge Between 24° N and 30°40′ N. *Nature* **34**, 427–431.

Seward, D., 1994, Fission Cracks Dates of Basalts from the North Fiji Basin, in L. W. Kroenke and J. V. Eade (eds.), "Basin Formation, Ridge Crest Processes and Metalogenesis in the North Fiji Basin", *Circum Pacific Council for Energy and Mineral Resources, Earth Science Series* **12**, 151–153.

Tanahashi, M., Kisimoto, K., Joshima, M., Jarvis, P., Iwabuchi, Y., Ruellan, E., and Auzende, J. M., 1994, 800 km Long N–S Spreading System of the North Fiji Basin. *Marine Geology, Special Issue*, (Starmer project: J. M. Auzende and Urabe T., eds.), 5–24.

Tiffin, D. L., Clarke, J. H., Hill, P., Jarvis, P., Johnson, D., Maillet, P., Parson, L., and Price, R., 1991, GLORIA Data from the North Fiji and Lau Basins: A Summary of Results. *Starmer Symposium*, Nouméa, abstract.

Von Stackelberg, U. and Rad, U. von, 1990, Geological Evolution and Hydrothermal Activity in the Lau and North Fiji Basins (Sonne Cruise SO-35)- a synthesis. *Geol. Jb.* **92**, 629–660.

Wessel, P. and Smith, W. H. F., 1991, Free Software Helps Map and Display Data, *EOS trans. AGU* **72**, 441, 445–446, 1991.

Woodhall, D., 1987, Geology of Rotuma, *Miner. Res. Dept. Fiji Bull.* **8**, 40 p.